

Supplementary Information

“Moraine crest or slope: an analysis of the effects of boulder position on cosmogenic exposure age”

Tomkins *et al.* (2020)

link to doi here

1 | Description

This supplementary file describes the contents of the following data tables:

1. “**Supplementary_Table_1_10Be.csv**”. This file includes ^{10}Be sample information used for TCN exposure age calculation. The data are listed in the format required for the CRONUS Earth Web Calculator (Version 2.0; Marrero et al. (2016), available at: <http://cronus.cosmogenicnuclides.rocks/2.0/>). Required variables and their descriptions are available here: <http://cronus.cosmogenicnuclides.rocks/2.0/html/al-be/CRONUScalc26Al10BeTemplate.xlsx>, with additional information in Section 2.1.
2. “**Supplementary_Table_2_36Cl.csv**”. This file includes ^{36}Cl sample information used for TCN exposure age calculation, in the format described above. Required variables and their descriptions are available here: <http://cronus.cosmogenicnuclides.rocks/2.0/html/cl/CRONUScalc36ClTemplate.xlsx>, with additional information in Section 2.1.
3. “**Supplementary_Table_3_SH.csv**”. This file includes sample information for all boulders sampled using the Schmidt hammer ($n = 645$). Variable names and calculation steps are described in Section 2.2.

These files have been made available with the accompanying paper: *link to doi here*. These files, and relevant code (R, Python), are also available on Github: https://github.com/matt-tomkins/moraine_paper_2020.

2 | Variable names

2.1 “Supplementary Tables 1-2”

Columns [5:35] (^{10}Be) and [5:83] (^{36}Cl) are in the format required by the CRONUS Earth Web Calculator (Marrero et al., 2016). The remaining variables are described below:

Group

Identifier to distinguish different exposure age groups, as described below:

- “Calibration *dataset*” = The 52 ^{10}Be dated surfaces used in Tomkins et al. (2018a).
- “Calibration *outlier*” = Outliers ($n = 2$; *see* Fig. 2.1A-B), excluded by Tomkins et al. (2018a). These samples are likely compromised by prior exposure (inheritance). These include sample CAC28 from the Cometa d’Espagne cirque (Crest et al., 2017), which is proximal (~2 m) to three tightly clustered bedrock ages (c. 11 - 12 ka; mean squared weighted deviation [MSWD] = 0.094). Similarly, sample ICM04 from the Malniu catchment (Pallàs et al., 2010) is proximal (~10m) to three dated moraine boulders (c. 40 - 50 ka; MSWD = 0.945). When these outliers are removed, both of these data sets are internally consistent (MSWD < 1).
- “Calibration *new*” = This includes two additional ^{10}Be ages from the Noguera Ribagorçana (MUL01 and MUL03; Pallàs et al., 2006) which were sampled with the Schmidt hammer during recent fieldwork (*see* Fig. 2.1C-D).
- “New moraine samples” = This includes all ^{10}Be and ^{36}Cl samples from the studied moraines ($n = 19$; Pallàs et al., 2006; Rodés, 2008; Palacios et al., 2015), of which 15 were sampled with the Schmidt hammer.

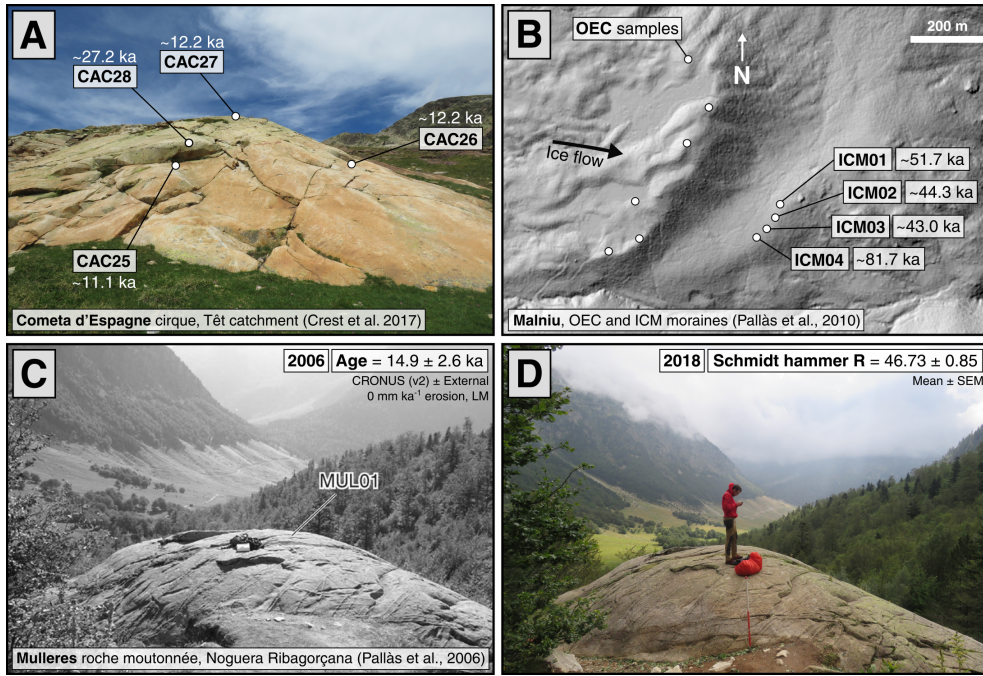


Figure 2.1: Outliers (A-B) and new calibration data (C-D) for the Pyrenean TCN-SH calibration curve (Tomkins et al., 2018a). (A) Outlier sample CAC28 from the Cometa d'Espagne cirque (Crest et al., 2017). (B) Outlier sample ICM04 from Malniu (Pallàs et al., 2010). (C) Sample photograph (2006) for new calibration sample MUL01 from the Noguera Ribagorçana (Pallàs et al., 2006) and its calculated surface exposure age (\pm external age uncertainty; CRONUS Earth Web Calculator, Marrero et al., 2016; 0 mm ka^{-1} erosion, LM scaling scheme). (D) Sample photograph for MUL01 (2018), with its corresponding mean Schmidt hammer R-value (\pm standard error of the mean).

Landform/Region

Name of the associated moraine, or sampling region.

Publication

Name of publication (Pallàs et al., 2006, 2010; Rodés, 2008; Delmas et al., 2008; Palacios et al., 2015; Crest et al., 2017).

SH_Mean

Mean of 30 Schmidt hammer R-values. No outliers were removed following Niedzielski et al. (2009).

SH_SEM

Standard error of the mean of 30 Schmidt hammer R-values.

SH_Sample_Name

If this surface was resampled with the Schmidt hammer, the corresponding sample name is listed here.

CRONUS_Age [Year_Month_Day] The sample exposure age (ka), and the calculation date.

CRONUS_Internal [Year_Month_Day] The internal exposure age uncertainty (ka), and the calculation date.

CRONUS_External [Year_Month_Day] The external exposure age uncertainty (ka), and the calculation date.

2.2 “Supplementary Table 3”

Sample name

Unique identifier for each boulder.

Landform

Name of the associated moraine, following the prior work of Pallàs et al. (2006), Rodés (2008) and Palacios et al. (2015).

Sub-Landform

Identifier to distinguish between the outer and inner Soum d’Ech moraines.

Latitude_DD

Sample latitude in decimal degrees (°).

Longitude_DD

Sample longitude in decimal degrees (°).

Elevation_m

Sample elevation in metres above sea level (m a.s.l.).

SH_Mean

Mean of 30 Schmidt hammer R-values. No outliers were removed following Niedzielski et al. (2009).

SH_MAD

Mean absolute deviation of 30 Schmidt hammer R-values.

SH_SEM

Standard error of the mean of 30 Schmidt hammer R-values.

TCN_Sample_Name

If this boulder has previously been dated using ^{10}Be or ^{36}Cl , the name is listed here.

Calibrated_Age_ka

Calibrated exposure age of the boulder (ka), calculated through interpolation of the TCN-SH calibration curve (*see* Fig. 2.2). This curve is derived from orthogonal distance regression (ODR; Boggs and Rogers, 1990b) and is based on 54 ^{10}Be dated granite and granodiorite surfaces from the Pyrenees (Pallàs et al., 2006, 2010; Delmas et al., 2008; Crest et al., 2017) and their corresponding Schmidt hammer R-values

(Tomkins et al., 2018a). ODR incorporates errors in both the independent and dependent variables, and here utilises ^{10}Be external age uncertainty and the standard error of the mean (SEM) of the Schmidt hammer R-values.

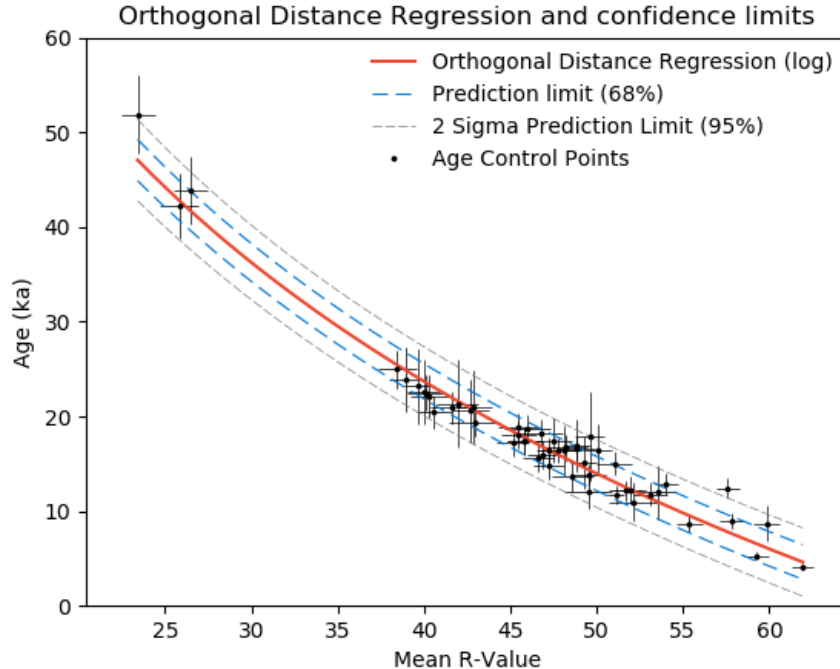


Figure 2.2: ODR TCN-SH calibration curve, based on 54 ^{10}Be dated granite and granodiorite surfaces from the Pyrenees.

This approach has now been implemented on SHED-Earth (<http://shed.earth>), an online calculator developed to enable wider and more consistent application of our approach (Tomkins et al., 2018b).

Calibrated_Uncertainty_ka

The associated uncertainty (ka), derived from a 1σ prediction limit. This prediction limit was calculated using the ODR covariance matrix (Boggs and Rogers, 1990a). The code for this analysis is available on Github (<https://github.com/jonnyhuck/shed-earth>).

A_axis_cm

Length of the longest boulder axis (cm).

B_axis_cm

Length of the intermediate boulder axis (cm).

C_axis_cm

Length of the shortest boulder axis (cm).

Ground_Height_cm

Maximum height of boulder above the ground (cm).

Volume_m3

Approximate volume of boulder (V , m³), calculated as the product of the axis lengths (m) as follows:

$$V = ABC$$

Surface_area_m2

Approximate surface area of boulder (S ; m²), calculated from the axis lengths (m) as follows:

$$S = 2(AB) + 2(AC) + 2(BC)$$

Sphericity

Boulder sphericity (ψ), as defined by Wadell (1935), calculated using boulder volume (V) and surface area (S) as follows:

$$\Psi = \frac{\pi^{\frac{1}{3}}(6S)^{\frac{2}{3}}}{A}$$

Mass_Tonnes

Approximate mass of the boulder in tonnes (T), calculated using boulder volume (V) and assuming a bulk density of 2.69 g cm³(D) as follows:

$$T = VD$$

Landform_Age_ka

Age of the landform (ka), calculated using the Probabilistic Cosmogenic Age Analysis Tool (P-CAAT Version 1.0; Dortch et al., 2019). This method utilises non-linear curve fitting and a Monte Carlo style approach to isolate component Gaussian distributions to account for positive (prior exposure) and negative skew (incomplete exposure) of age datasets and builds on previous work of Dortch et al. (2013) and Murari et al. (2014).

Landform_Uncertainty_ka

Uncertainty (ka) of the landform age. This estimate is derived from the 1σ bounds of the isolated component Gaussian distribution.

Relative_Difference_ka

Relative difference between the calibrated exposure age of the boulder and the age of the landform (ka).

Absolute_Difference_ka

Absolute difference between the calibrated exposure age of the boulder and the age of the landform (ka).

Class_95

Boulder class (“Young”, “Good”, “Old”) as defined by the 2σ uncertainty bounds (U ; ~95%) of the landform age (L , ka). These are distinguished as follows:

$$Young < L - U$$

$$Good \geq L - U \mid \leq L + U$$

$$Old > L + U$$

General_Class_95

Boulder class (“Good”, “Bad”) as defined by the 2σ uncertainty bounds (U ; ~95%) of the landform age (L , ka). These are distinguished as follows:

$$Good \geq L - U \mid \leq L + U$$

$$Bad < L - U \mid > L + U$$

Moraine_Group

Boulder group, either moraine crest (C), the inner ice-proximal slope (IS) or the outer ice-distal slope (OS).

AB | AC_Ratio

Ratio of longest (*A*) to intermediate (*B*) or shortest axes (*C*).

Moss

Approximate boulder coverage by moss or surface vegetation (0%, 20%, 40%, 60%, 80%, 100%). Note, Schmidt hammer sampling was conducted in areas free of moss or surface vegetation.

Lichen

Binary category for lichen coverage (0 = Lichen absent, 1 = Lichen present). Note, Schmidt hammer sampling was conducted in lichen free areas following Matthews and Owen (2008).

Embedded

Approximate percentage of boulder embedded in ground (0%, 20%, 40%, 60%, 80%, 100%).

Angularity

Boulder morphology: Angular (A), Sub-angular (SA), Sub-rounded (SR) or Rounded (R).

Fractured

Qualitative assessment of the degree of fracturing, defined as follows:

- 0 = no fractures.
- 0.25 = minor fractures.
- 0.5 = some fractures.
- 0.75 = major fractures.
- 1 = predominantly fractured.

Note, Schmidt hammer sampling was conducted away from fractures or surface discontinuities following Williams and Robinson (1983).

Matrix

Characteristics of the underlying material, defined as follows:

- 0 = soil or sediment (i.e. matrix supported)
- 0.5 = combination of matrix and clast support e.g. sediment and boulders *or* cobbles with tightly packed sediment.
- 1 = boulders or cobbles (i.e. clast supported)

Crest_polyline_dist_m

Distance between the boulder and the moraine crest (m), digitised as a polyline (.shp) along the centre of the moraine crest.

Crest_polygon_dist_m

Distance between the boulder and the moraine crest (m), digitised as a polygon (.shp) incorporating the entire moraine crest area.

Front_dist_m

Distance between the boulder and the front of the moraine (m).

Slope_Angle_deg

Angle ($^{\circ}$) of the underlying slope.

Bibliography

- Boggs, P. T. and Rogers, J. E. The Computation and Use of the Asymptotic Covariance Matrix for Measurement Error Models. Technical Report Internal Report 89-4102, National Institute of Standards and Technology, Gaithersburg, MD, Applied and Computational Mathematics Division.
- Boggs, P. T. and Rogers, J. E. Orthogonal distance regression. In "*Statistical analysis of measurement error models and applications: proceedings of the AMS-IMS-SIAM joint summer research conference held June 10-16, 1989*," volume 12, page 186. 1990, doi: 10.6028/nist.ir.89-4197.
- Crest, Y., Delmas, M., Braucher, R., Gunnell, Y., and Calvet, M. Cirques have growth spurts during deglacial and interglacial periods: Evidence from ^{10}Be and ^{26}Al nuclide inventories in the central and eastern Pyrenees. *Geomorphology*, 278:60–77, 2017, doi:10.1016/j.geomorph.2016.10.035.
- Delmas, M., Gunnell, Y., Braucher, R., Calvet, M., and Bourlès, D. Exposure age chronology of the last glaciation in the eastern Pyrenees. *Quaternary Research*, 69(2):231–241, 2008, doi:10.1016/j.yqres.2007.11.004.
- Dortch, J., Saha, S., Tomkins, M. D., Murari, M. K., Schoenbohm, L. M., and Curl, D. Probability-based interpretation of terrestrial cosmogenic radionuclide ages: P-CAAT, a tool for the ages. AGU. 2019, doi: <https://agu.confex.com/agu/fm19/meetingapp.cgi/Paper/502207>.
- Dortch, J. M., Owen, L. A., and Caffee, M. W. Timing and climatic drivers for glaciation across semi-arid western Himalayan–Tibetan orogen. *Quaternary Science Reviews*, 78:188–208, 2013, doi:10.1016/j.quascirev.2013.07.025.
- Marrero, S. M., Phillips, F. M., Borchers, B., Lifton, N., Aumer, R., and Balco, G. Cosmogenic nuclide systematics and the CRONUScalc program. *Quaternary Geochronology*, 31:160–187, 2016, doi:10.1016/j.quageo.2015.09.005.
- Matthews, J. A. and Owen, G. Endolithic lichens, rapid biological weathering and schmidt hammer r-values on recently exposed rock surfaces: storbreen glacier foreland, jotunheimen, norway. *Geografiska Annaler: Series A, Physical Geography*, 90(4):287–297, 2008, doi:10.1111/j.1468-0459.2008.00346.x.
- Murari, M. K., Owen, L. A., Dortch, J. M., Caffee, M. W., Dietsch, C., Fuchs, M., Haneberg, W. C., Sharma, M. C., and Townsend-Small, A. Timing and climatic drivers for glaciation across monsoon-influenced regions of the Himalayan–Tibetan orogen. *Quaternary Science Reviews*, 88:159–182, 2014, doi:10.1016/j.quascirev.2014.01.013.
- Niedzielski, T., Migoń, P., and Placek, A. A minimum sample size required from Schmidt hammer measurements. *Earth Surface Processes and Landforms*, 34(13):1713–1725, 2009, doi:10.1002/esp.1851.
- Palacios, D., Gómez-Ortiz, A., Andrés, N., Vázquez-Selem, L., Salvador-Franch, F., and Oliva, M. Maximum extent of Late Pleistocene glaciers and last deglaciation of La Cerdanya mountains, Southeastern Pyrenees. *Geomorphology*, 231:116–129, 2015, doi:10.1016/j.geomorph.2014.10.037.
- Pallàs, R., Rodés, Á., Braucher, R., Carcaillet, J., Ortuño, M., Bordonau, J., Bourlès, D., Vilaplana, J. M., Masana, E., and Santanach, P. Late Pleistocene and Holocene glaciation in the Pyrenees: a critical review and new evidence from ^{10}Be exposure ages, south-central Pyrenees. *Quaternary Science Reviews*, 25(21):2937–2963, 2006, doi:10.1016/j.quascirev.2006.04.004.
- Pallàs, R., Rodés, Á., Braucher, R., Bourlès, D., Delmas, M., Calvet, M., and Gunnell, Y. Small, isolated glacial catchments as priority targets for cosmogenic surface exposure dating of Pleistocene climate fluctuations, southeastern Pyrenees. *Geology*, 38(10):891–894, 2010, doi:10.1130/G31164.1.
- Rodés, Á. *La última deglaciación en los pirineos: de superficies de exposición mediante ^{10}Be , y modelado numérico de paleoglaciares*. <http://purl.org/dc/dcmitype/Text>, Universitat de Barcelona. Pages: 1.
- Tomkins, M. D., Dortch, J. M., Hughes, P. D., Huck, J. J., Stimson, A. G., Delmas, M., Calvet, M., and Pallàs, R. Rapid age assessment of glacial landforms in the Pyrenees using Schmidt hammer exposure dating (SHED). *Quaternary Research*, 90(1):26–37, 2018, doi:10.1017/qua.2018.12.

Tomkins, M. D., Huck, J. J., Dortch, J. M., Hughes, P. D., Kirkbride, M. P., and Barr, I. D. Schmidt Hammer exposure dating (SHED): Calibration procedures, new exposure age data and an online calculator. *Quaternary Geochronology*, 44:55–62, 2018, doi:10.1016/j.quageo.2017.12.003.

Wadell, H. Volume, Shape, and Roundness of Quartz Particles. *The Journal of Geology*, 43(3):250–280, 1935, doi:10.1086/624298. Publisher: The University of Chicago Press.

Williams, R. B. G. and Robinson, D. A. The effect of surface texture on the determination of the surface hardness of rock using the schmidt hammer. *Earth Surface Processes and Landforms*, 8(3):289–292, 1983, doi:10.1002/esp.3290080311.